MARKOV RANDOM FIELDS FOR JOINT UNMIXING AND SEGMENTATION OF HYPERSPECTRAL IMAGES

Olivier Eches, Nicolas Dobigeon and Jean-Yves Tourneret

University of Toulouse, IRIT/INP-ENSEEIHT, 2 rue Camichel, 31071 Toulouse cedex 7, France

{olivier.eches,nicolas.dobigeon,jean-yves.tourneret}@enseeiht.fr

ABSTRACT

This paper studies a new Bayesian algorithm for the unmixing of hyperspectral images. The proposed Bayesian algorithm is based on the well-known linear mixing model (LMM). Spatial correlations between pixels are introduced using hidden variables, or *labels*, and modeled via a Potts-Markov random field. We assume that the pure materials (or *endmembers*) contained in the image are known a priori or have been extracted by using an endmember extraction algorithm. The mixture coefficients (referred to as *abundances*) of the whole hyperspectral image are then estimated by using a hierarchical Bayesian algorithm. A reparametrization of the abundances is considered to handle the physical constraints associated to these parameters. Appropriate prior distributions are assigned to the other parameters and hyperparameters associated to the proposed model. To alleviate the complexity of the resulting joint distribution, a hybrid Gibbs algorithm is developed, allowing one to generate samples that are asymptotically distributed according to the full posterior distribution of interest. The generated samples are finally used to estimate the unknown model parameters. Simulations on synthetic data illustrate the performance of the proposed method.

***Index Terms*—** Bayesian inference, Monte Carlo methods, spectral unmixing, hyperspectral images, Markov random fields.

1. INTRODUCTION

The unmixing problem is a very crucial step in hyperspectral image analysis. It consists of decomposing a measured pixel reflectance into mixtures of pure spectra, known as *endmembers*, whose fractions are referred to as *abundances*. A very common assumption in the unmixing framework is to consider the image pixels as linear combinations of these endmembers. More precisely, the so-called linear mixing model (LMM) assumes that the L-spectrum $\boldsymbol{y}_p = [y_{p,1}, \ldots, y_{p,L}]^T$ of a mixed pixel is modeled as

$$\boldsymbol{y}_p = \boldsymbol{M}\boldsymbol{a}_p + \boldsymbol{n}_p, \qquad (1)$$

where $\boldsymbol{M} = [\boldsymbol{m}_1, \ldots, \boldsymbol{m}_R]$ is a known $L \times R$ matrix containing the L-spectra of the endmembers, $\boldsymbol{a}_p$ is the $R \times 1$ abundance vector associated to the piwel p, R is the number of endmembers that are present in the image and $\boldsymbol{n}_p$ is the independent and identically distributed (i.i.d.) zero-mean Gaussian noise sequence with variance s_p^2. Due to obvious physical considerations, the abundances satisfy positivity and sum-to-one constraints. In this work, the endmember spectral signatures are assumed to be known and can be obtained from a spectral library or by an endmember extraction algorithm (EEA), such as the Pixel Purity Index (PPI) [1], N-finder (N-FINDR) [2] or the vertex component analysis (VCA) [3]. After identification of these signatures, the corresponding abundances are estimated using an *inversion* step. Many algorithms have been developed for this inversion. For instance, these algorithms can be based on Bayesian inference [4] or on the fully constrained least squares (FCLS) method [5]. However, all these inversion strategies have been developed in a pixel-by-pixel context. Consequently, they do not exploit the possible spatial correlations between the different pixels of the hyperspectral image.

We propose in this paper to exploit the correlations between the pixel of the image to derived a new unmixing procedure. More precisely, the Bayesian unmixing strategy developed in [4] is generalized to take into account spatial correlations between the pixels of an hyperspectral image. First, the image is partitioned into homogeneous regions in which the abundance vectors have the same first and second order statistics (means and covariances). This implies an implicit image classification modeled by hidden labels whose spatial dependencies are modeled by a Potts-Markov random field [6] (a particular case of Markov random fields (MRF)). Popularized by Geman [7], the MRFs are a very useful tool to describe neighborhood dependance between image pixels and have been used for hyperspectral image classification [8]. Appropriate prior distributions with unknown means and variances depending on the pixel class are chosen for the abundance vectors that are reparametrized in a much more flexible way than in [4]. The associated hyperparameters are assigned non-informative prior distributions. The joint posterior distribution is then computed from the likelihood and these prior distributions. This posterior is too complex to derive the classical Bayesian estimators such as the MMSE and MAP estimators. Thus we propose to use Markov chain Monte Carlo (MCMC) methods to generate samples asymptotically distributed according to the joint posterior of interest. These samples are then used to estimate the unknown model parameters.

The remainder of the paper is organized as follows. Section 2 presents the proposed hierarchical Bayesian model for hyperspectral image unmixing. Section 3 studies an MCMC strategy that generates samples according to the resulting posterior. Section 4 shows simulation results on synthetic data. Conclusions are reported in Section 5.

2. HIERARCHICAL BAYESIAN MODEL

Before presenting the likelihood and prior distributions for this unmixing problem, the image partitioning and the reparametrization of the abundance coefficients are formally described.

2.1. Introducing spatial dependencies between the image pixel abundances

This paper assumes that the abundances of a given pixel are *a priori* close to the abundances of its neighboring pixels. Let the image be partitioned into K regions or *classes* and $\mathcal{I}_k \subset \{1, \dots, K\}$ denotes the subset of pixel indexes belonging to the kth class. We introduce a label vector denoted as $\boldsymbol{z} = [z_1, \dots, z_P]^T$ where P is the total number of pixels and $z_p \in \{1, \dots, K\}$ allows one to identify the class to which each pixel p belongs ($p = 1, \dots, P$). In other words $z_p = k$ if and only if $p \in \mathcal{I}_k$.

In each class, the abundance vectors share the same mean and variance. As explained above, the abundances have to satisfy positivity and sum-to-one constraints for each pixel p

$$\left\{ \begin{array}{l} a_{r,p} \geq 0, \forall r = 1, \dots, R, \\ \sum_{r=1}^{R} a_{r,p} = 1, \end{array} \right. \tag{2}$$

where $\boldsymbol{a}_p = [a_{1,p}, \dots, a_{R,p}]^T$. Following the strategy in [9], we propose to reparametrize the abundance coefficients by using random *logistic* coefficients $\boldsymbol{t}_p = [t_{1,p} \dots, t_{R,p}]^T$ such as

$$a_{r,p} = \frac{\exp(t_{r,p})}{\sum_{r=1}^{R} \exp(t_{r,p})}. \tag{3}$$

This reparametrization ensures positivity and sum-to-one constraints for the abundances. We assume that the distribution of the logistic coefficients $\boldsymbol{t}_p,\ p \in \mathcal{I}_k$ for the kth class is a Gaussian distribution, i.e., fully characterized by a mean vector $\boldsymbol{\psi}_k$ and a covariance matrix $\boldsymbol{\Sigma}_k$.

2.2. Likelihood

First, the unknown parameter vector associated to the LMM unmixing strategy is defined as $\boldsymbol{\Theta} = \{\boldsymbol{T}, \boldsymbol{z}, s\}$, where $\boldsymbol{s} = \left[s_1^2, \dots, s_P^2\right]^T$ is the noise variance vector, $\boldsymbol{z}$ is the label vector and $\boldsymbol{T} = [\boldsymbol{t}_1, \dots, \boldsymbol{t}_P]$ with $\boldsymbol{t}_p = [\boldsymbol{t}_{1,p}, \dots, \boldsymbol{t}_{R,p}]^T$ ($p = 1, \dots, P$) is the logistic coefficient matrix used for the abundance reparametrization. The additive white Gaussian noise sequence of the LMM allows one to write[1] $\boldsymbol{y}_p | \boldsymbol{t}_p, s_p^2 \sim \mathcal{N}\left(\boldsymbol{M}\boldsymbol{a}_p(\boldsymbol{t}_p), s_p^2 \boldsymbol{I}_L\right)$ ($p = 1, \dots, P$). Therefore the likelihood function of $\boldsymbol{y}_p$ can be expressed as

$$f\left(\boldsymbol{y}_p \,|\boldsymbol{t}_p, s_p^2\right) = \left(\frac{1}{2\pi s_p^2}\right)^{\frac{L}{2}} \exp\left[-\frac{\|\boldsymbol{y}_p - \boldsymbol{M}\boldsymbol{a}_p(\boldsymbol{t}_p)\|^2}{2s_p^2}\right], \tag{4}$$

where $\|\boldsymbol{x}\| = \sqrt{\boldsymbol{x}^T\boldsymbol{x}}$ is the standard ℓ_2 norm. By assuming independence between the noise vectors $\boldsymbol{n}_p$ ($p = 1, \dots, P$), the likelihood of the P image pixels is

$$f\left(\boldsymbol{Y}|\boldsymbol{T}, \boldsymbol{s}\right) = \prod_{p=1}^{P} f\left(\boldsymbol{y}_p|\boldsymbol{t}_p, s_p^2\right). \tag{5}$$

2.3. Parameter priors

This section introduces the prior distributions of the unknown parameters and their associated hyperparameters in the proposed hierarchical Bayesian framework.

2.3.1. Label prior

The spatial correlation between the image pixels can be represented by using MRFs as stated above. The MRFs allow one to define a symmetric relation between one pixel and its nearby neighbors through the use of integer variables (the labels in our study). More specifically, the prior distribution of the label vector $\boldsymbol{z} = [z_1, \dots, z_P]^T$ is a Potts-Markov random field, as in [8]. Considering a pixel p and its 4 nearby neighbors (first order neighborhood), the resulting prior distribution for the label vector can be written as

$$f(\boldsymbol{z}) \propto \exp\left[\sum_{p=1}^{P} \sum_{p' \in \mathcal{V}(p)} \beta\delta(z_p - z_{p'})\right], \tag{6}$$

where $\propto$ means "proportional to", $\mathcal{V}(p)$ is the first order neighborhood, β is the *granularity* coefficient (assumed to be known in this study) and $\delta(\cdot)$ is the Kronecker function

$$\delta(x) = \left\{ \begin{array}{ll} 1, & \text{if } x = 0, \\ 0, & \text{otherwise.} \end{array} \right.$$

2.3.2. Logistic coefficients and noise variance prior

For a given pixel p and by assuming independence between the logistic coefficients $t_{1,p}, \dots, t_{R,p}$, the prior distribution for the vector $\boldsymbol{t}_p = [t_{1,p}, \dots, t_{R,p}]^T$ is the following Gaussian distribution

$$f\left(\boldsymbol{t}_p | z_p = k, \boldsymbol{\psi}_k, \boldsymbol{\Sigma}_k\right) \sim \mathcal{N}\left(\boldsymbol{\psi}_k, \boldsymbol{\Sigma}_k\right) \tag{7}$$

parameterized by the hyperparameter vector $\boldsymbol{\psi}_k = [\psi_{1,k}, \dots, \psi_{R,k}]^T$ and by the $R \times R$ diagonal matrix $\boldsymbol{\Sigma}_k = \operatorname{diag}\left(\sigma_{r,k}^2\right)$ whose diagonal elements are $\sigma_{r,k}^2$ for $r = 1, ..., R$. Note that, as highlighted in paragraph 2.1, the mean vector $\boldsymbol{\psi}_k$ and the covariance matrix $\boldsymbol{\Sigma}_k$ of the logistic coefficient vector $\boldsymbol{t}_p$ both depend on the region k. By assuming prior independence between the P vectors $\boldsymbol{t}_1, \dots, \boldsymbol{t}_P$, the full posterior distribution for the logistic coefficient matrix $\boldsymbol{T}$ is

$$f\left(\boldsymbol{T}|\boldsymbol{\Psi}, \boldsymbol{\Sigma}\right) = \prod_{k=1}^{K} \prod_{p \in \mathcal{I}_k} f\left(\boldsymbol{t}_p | z_p = k, \boldsymbol{\psi}_k, \boldsymbol{\Sigma}_k\right), \tag{8}$$

with $\boldsymbol{\Psi} = [\boldsymbol{\psi}_1, \dots, \boldsymbol{\psi}_K]$ and $\boldsymbol{\Sigma} = \{\boldsymbol{\Sigma}_1, \dots, \boldsymbol{\Sigma}_K\}$.

A conjugate exponential distribution is assigned to the inverse noise variance,

$$s_p^{-2} | \delta \sim \mathcal{E}(\delta) \tag{9}$$

where δ is an adjustable hyperparameter. Assuming independence between the noise variances s_p^2, ($p = 1, \dots, P$), the full prior distribution for $\boldsymbol{s} = \left[s_1^2, \dots, s_P^2\right]^T$ can be expressed as

$$f\left(\boldsymbol{s}|\delta\right) = \prod_{p=1}^{P} f\left(s_p^2|\delta\right). \tag{10}$$

Hierarchical Bayesian algorithms consist of jointly estimating the model parameters and hyperparameters. These algorithms require to define prior distributions for the unknown hyperparameters. It is the purpose of the next section.

2.4. Hyperparameter priors

We propose to define prior distributions for the logistic coefficient means $\psi_{r,k}$ and variances $\sigma_{r,k}^2$ as conjugate Gaussian and inverse-gamma distributions, i.e.,

$$\begin{array}{l} \psi_{r,k} | \upsilon^2 \sim \mathcal{N}\left(0, \upsilon^2\right) \\ \sigma_{r,k}^2 | \xi, \gamma \sim \mathcal{IG}(\xi, \gamma) \end{array} \tag{11}$$

where υ^2 is an adjustable hyperparameter and ξ and γ have been fixed to $\xi = 1$ and $\gamma = 5$ (in order to obtain a large variance).

[1] Note that the dependence of the abundance vector $\boldsymbol{a}_p$ on the logistic coefficient vector $\boldsymbol{t}_p$ throught (3) is explicitly mentioned by denoting $\boldsymbol{a}_p = \boldsymbol{a}_p(\boldsymbol{t}_p)$.

Moreover, we assign Jeffreys' priors to the hyperparameters δ and υ^2 defined as

$$f(\delta) \propto \frac{1}{\delta}\mathbf{1}_{\mathbb{R}^+}(\delta), \quad f(\upsilon^2) \propto \frac{1}{\upsilon^2}\mathbf{1}_{\mathbb{R}^+}(\upsilon^2). \tag{12}$$

By assuming *a priori* independence between the individual hyperparameters, the full hyperprior can be obtained for the hyperparameter vector $\Omega = \left\{\boldsymbol{\Psi}, \boldsymbol{\Sigma}, \upsilon^2, \delta\right\}$

$$f(\Omega) \propto f(\delta) f(\upsilon^2) \prod_{k=1}^{K}\prod_{r=1}^{R} f(\psi_{r,k}|\upsilon^2) f(\sigma_{r,k}^2). \tag{13}$$

2.5. Joint distribution

The likelihood and the priors define above allow us to express the joint posterior distribution using the hierarchical structure

$$\begin{aligned} f(\boldsymbol{\Theta}, \Omega|\boldsymbol{Y}) &= f(\boldsymbol{Y}|\boldsymbol{\Theta}) f(\boldsymbol{\Theta}|\Omega) f(\Omega) \\ &\propto \prod_{p=1}^{P}\left(\frac{1}{s_p^2}\right)^{\frac{L}{2}} \exp\left[-\frac{\|\boldsymbol{y}_p - \boldsymbol{M}\boldsymbol{a}_p(\boldsymbol{t}_p)\|^2}{2s_p^2}\right] \\ &\times \exp\left[\sum_{p=1}^{P}\sum_{p'\in\mathcal{V}(p)} \beta\delta(z_p - z_{p'})\right] \\ &\times \delta^{P-1}\prod_{p=1}^{P}\left(\frac{1}{w_p^2}\right)^{\nu+1}\exp\left(-\frac{\delta}{w_p^2}\right)\left(\frac{1}{\upsilon^2}\right)^{\frac{RK}{2}+1} \\ &\times \prod_{r,k}\frac{1}{\sigma_{r,k}^{n_k+1}}\exp\left[-\left(\frac{\psi_{r,k}^2}{2\upsilon^2} + \frac{2\gamma + \sum_{p\in\mathcal{I}_k}(t_{r,p} - \psi_{r,k})^2}{2\sigma_{r,k}^2}\right)\right] \end{aligned} \tag{14}$$

with $n_k = \mathrm{card}(\mathcal{I}_k)$. Since the posterior distribution (14) is too complex to derive closed-form expressions for the MMSE and MAP estimators of $\boldsymbol{\Theta}$, a hybrid Gibbs sampler is employed to generate samples that are asymptotically distributed according to this distribution. The samples are then used to approximate the Bayesian estimators.

3. HYBRID GIBBS SAMPLER

The principle of the Gibbs sampler is to iteratively generate samples distributed according to the conditional distributions of the distribution of interest. This section derives the conditional distributions associated to (14).

3.1. Conditional distribution of the label vector $\boldsymbol{z}$

For each pixel p ($p = 1, \ldots, P$), the class label z_p is a discrete random variable whose conditional distribution is fully characterized by the probabilities expressed as

$$\begin{aligned} \mathrm{P}\left[z_p = k|\boldsymbol{z}_{\text{-}p}, \boldsymbol{t}_p, \boldsymbol{\psi}_k, \boldsymbol{\Sigma}_k\right] &\propto \\ |\boldsymbol{\Sigma}_k|^{-1/2} &\exp\left[-\frac{1}{2}\left(\boldsymbol{t}_p - \boldsymbol{\psi}_k\right)^T \boldsymbol{\Sigma}_k^{-1}\left(\boldsymbol{t}_p - \boldsymbol{\psi}_k\right)\right] \\ &\times \exp\left[\sum_{p=1}^{P}\sum_{p'\in\mathcal{V}(p)}\beta\delta(z_p - z_{p'})\right] \end{aligned} \tag{15}$$

with $|\boldsymbol{\Sigma}_k| = \prod_{r=1}^{R}\sigma_{r,k}^2$, $k = 1, ..., K$ (K is the number of classes) and $\boldsymbol{z}_{\text{-}p}$ denotes the vector $\boldsymbol{z}$ whose pth element has been removed. Since this distribution is discrete, the samples are drawn by generating a discrete value in the finite set $\{1, \ldots, K\}$ with the probabilities (15) as detailed in [10].

3.2. Conditional distribution of logistic coefficient matrix $\boldsymbol{T}$

For a given pixel p, the conditional distribution of $\boldsymbol{t}_p$ is

$$\begin{aligned} f\left(\boldsymbol{t}_p|z_p = k, \boldsymbol{\psi}_k, \boldsymbol{\Sigma}_k, \boldsymbol{y}_p, s_p^2\right) &\propto \\ \left(\frac{1}{s_p^2}\right)^{\frac{L}{2}} &\exp\left\{-\frac{1}{2s_p^2}\left\|\boldsymbol{y}_p - \boldsymbol{M}\boldsymbol{a}_p(\boldsymbol{t}_p)\right\|^2\right\} \\ \times |\boldsymbol{\Sigma}_k|^{-\frac{1}{2}} &\exp\left[-\frac{1}{2}\left(\boldsymbol{t}_p - \boldsymbol{\psi}_k\right)^T \boldsymbol{\Sigma}_k^{-1}\left(\boldsymbol{t}_p - \boldsymbol{\psi}_k\right)\right]. \end{aligned} \tag{16}$$

Since it is too difficult to generate samples according to this posterior distribution, a Metropolis-Hastings step is used with a Gaussian distribution as proposal distribution, following the strategy detailed in [10].

3.3. Conditional distributions of the noise variances

Considering each pixel p, $s_p^2|\boldsymbol{y}_p, \boldsymbol{t}_p, \delta$ is distributed according to the inverse-Gamma distribution

$$s_p^2|\boldsymbol{y}_p, \boldsymbol{t}_p, \delta \sim \mathcal{IG}\left(\frac{L}{2} + 1, \frac{\|\boldsymbol{y}_p - \boldsymbol{M}\boldsymbol{a}_p(\boldsymbol{t}_p)\|^2}{2} + \delta\right). \tag{17}$$

3.4. Conditional distributions of $\boldsymbol{\Psi}$ and $\boldsymbol{\Sigma}$

For each endmember r ($r = 1, \ldots, R$) and each class k ($k = 1, \ldots, K$) and by denoting $\bar{t}_{r,k} = \frac{1}{n_k}\sum_{p\in\mathcal{I}_k} t_{r,p}$, the conditional distributions of $\psi_{r,k}$ and $\sigma_{r,k}^2$ can be written as

$$\psi_{r,k}|\boldsymbol{z} = k, \boldsymbol{t}_r, \sigma_{r,k}^2, \upsilon^2 \sim \mathcal{N}\left(\frac{\upsilon^2 n_k \bar{t}_{r,k}}{\sigma_{r,k}^2 + \upsilon^2 n_k}, \frac{\upsilon^2\sigma_{r,k}^2}{\sigma_{r,k}^2 + \upsilon^2 n_k}\right) \tag{18}$$

$$\sigma_{r,k}^2|\boldsymbol{z} = k, \boldsymbol{t}_r, \psi_{r,k} \sim \mathcal{IG}\left(\frac{n_k}{2} + 1, \gamma + \sum_{p\in\mathcal{I}_k}\frac{(t_{r,p} - \psi_{r,k})^2}{2}\right). \tag{19}$$

3.5. Conditional distributions of υ^2 and δ

The conditional distributions of υ^2 and δ are respectively the following inverse-gamma and gamma distributions

$$\upsilon^2|\boldsymbol{\Psi} \sim \mathcal{IG}\left(\frac{RK}{2}, \frac{1}{2}\sum_{k=1}^{K}\boldsymbol{\psi}_k{}^T\boldsymbol{\psi}_k\right), \quad \delta|\boldsymbol{s} \sim \mathcal{G}\left(P, \sum_{p=1}^{P}\frac{1}{s_p^2}\right). \tag{20}$$

The proposed Gibbs sampler iteratively generates N_{MC} samples distributed according to (15), (16), (17), (18), (19) and (20). The first generated samples N_{bi} belonging to the so-called *burn-in* period are ignored whereas the last samples are used to estimate the unknown model parameters and hyperparameters. More precisely, the labels are estimated using the MAP estimator approximated by retaining the samples that maximizes the conditional distribution of $\boldsymbol{z}$. Then, the abundance vector must be estimated conditionally to the MAP estimates of the labels. The MMSE estimator employed can be approximated by averaging over the $N_{\mathrm{MC}} - N_{\mathrm{bi}}$ samples.

4. SIMULATION RESULTS ON SYNTHETIC DATA

The accuracy of the proposed unmixing algorithm has been tested on a 25×25 synthetic image with $K = 3$ different classes and $R = 3$ mixed components whose spectra ($L = 413$ spectral bands) are construction concrete, green grass and micaceous loam (extracted from

Table 1. Actual and estimated abundance mean and variance for each class.

	Class 1		Class 2		Class 3	
	$\mathrm{E}[\boldsymbol{a}_p]$	$\mathrm{Var}[a_{p,r}]$	$\mathrm{E}[\boldsymbol{a}_p]$	$\mathrm{Var}[a_{p,r}]$	$\mathrm{E}[\boldsymbol{a}_p]$	$\mathrm{Var}[a_{p,r}]$
Actual values	$[0.6, 0.3, 0.1]^T$	0.005	$[0.3, 0.5, 0.2]^T$	0.005	$[0.3, 0.2, 0.5]^T$	0.005
Estimated values (LMM)	$[0.58, 0.29, 0.13]^T$	0.0047	$[0.29, 0.49, 0.2]^T$	0.0055	$[0.31, 0.19, 0.49]^T$	0.0076

ENVI software library). A label map, represented in Fig. 1 (left), has been generated using a Potts-Markov field with $\beta = 1.1$. Then, the mean and variance for the abundances have been chosen for each class according to the values in Tab. 1. The generated abundance maps for the LMM are depicted in Fig. 2 (top). Note that a black (resp. white) pixel indicates a weak (resp. strong) value of the abundance coefficient. The noise variance was generated according to its prior distribution with $\delta = 1 \times 10^{-3}$, leading to a signal-to-noise ratio of 19dB. A number of $N_{\mathrm{MC}} = 5000$ iterations (with 500 burn-in iterations) was chosen for all results.

As mentioned previously, the samples generated by the Gibbs sampler allow us to determine the MMSE and MAP estimators of the model parameters. Fig. 1 (right) shows MAP estimates for the label vectors. The corresponding MMSE estimates of the abundances conditioned upon these estimated labels are depicted in Fig. 2 (bottom). Table 1 shows the estimated means and variances of the estimated abundances. The estimated classes, abundance coefficients and abundance mean vectors estimated by our algorithm are clearly in accordance with the actual values of these parameters. Note that the execution time of this simulation on a Core(TM)2Duo 2.66GHz was about 26 minutes.

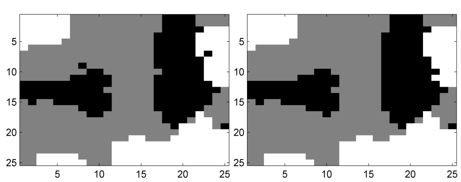

Fig. 1. Left: original labels. Right: labels estimated by the proposed hybrid Gibbs sampler.

5. CONCLUSIONS

This paper studied a new unmixing algorithm taking into account the spatial correlations between the pixels of an hyperspectral image. An additional hidden discrete variable (label) was introduced to identify several classes defined by homogeneous abundances (with common first and second order statistics). We derived the joint posterior distribution of the unknown parameters and hyperparameters associated to the proposed Bayesian linear mixing model and generated samples according to this posterior distribution using an hybrid Gibbs sampler. The generated samples were then used to estimate the abundance maps as well as the underlying image labels. The results obtained on simulated data are interesting. This algorithm has also been applied on real data. The results are given in [10]. The estimation of the granularity coefficient involved in Potts-Markov random fields is currently under investigation.

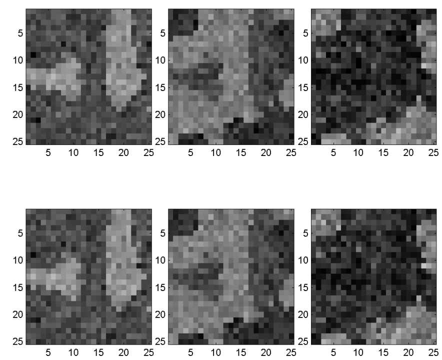

Fig. 2. Top: abundance maps of the 3 pure materials for LMM. Bottom: estimated abundance maps of the 3 pure materials from the LMM hybrid Gibbs sampler (from left to right: construction concrete, green grass, micaceous loam).

6. REFERENCES

[1] J. W. Boardman, F. A. Kruse, and R. O. Green, “Mapping target signatures via partial unmixing of AVIRIS data,” *Summaries of the Fifth Annual JPL Airborne Earth Science Workshop*, vol. 95, no. 1, pp. 23–26, 1995.

[2] M. E. Winter, “Fast autonomous spectral endmember determination in hyperspectral data,” in *Proc. 13th Int. Conf. on Applied Geologic Remote Sensing*, vol. 2, Vancouver, April 1999, pp. 337–344.

[3] J. M. Nascimento and J. M. Bioucas-Dias, “Vertex component analysis: a fast algorithm to unmix hyperspectral data,” *IEEE Trans. Geosci. and Remote Sensing*, vol. 43, no. 4, pp. 898–910, April 2005.

[4] N. Dobigeon, J.-Y. Tourneret, and C.-I Chang, “Semi-supervised linear spectral using a hierarchical Bayesian model for hyperspectral imagery,” *IEEE Trans. Signal Processing*, vol. 56, no. 7, pp. 2684–2696, July 2008.

[5] D. C. Heinz and C.-I Chang, “Fully constrained least squares linear spectral mixture analysis method for material quantification in hyperspectral imagery,” *IEEE Trans. Geosci. and Remote Sensing*, vol. 39, no. 3, pp. 529–545, March 2001.

[6] F. Wu, “The Potts model,” *Rev. Modern Phys.*, vol. 54, no. 1, pp. 235–268, Jan. 1982.

[7] S. Geman and D. Geman, “Stochastic relaxation, Gibbs distributions, and the Bayesian restoration of images,” *IEEE Trans. Patt. Anal. Mach. Intell.*, vol. 6, no. 6, pp. 721–741, Nov. 1984.

[8] N. Bali and A. Mohammad-Djafari, “Bayesian approach with hidden Markov modeling and mean field approximation for hyperspectral data analysis,” *IEEE Trans. Image Processing*, vol. 17, no. 2, pp. 217–225, Feb. 2008.

[9] K. Themelis and A. A. Rontogiannis, “A soft constrained MAP estimator for supervised hyperspectral signal unmixing,” in *Proc. of European Signal Processing Conf. (EUSIPCO)*, Lausanne, Switzerland, Aug. 2008.

[10] O. Eches, N. Dobigeon, and J.-Y. Tourneret, “Enhancing hyperspectral image unmixing with spatial correlations,” *IEEE Trans. Geosci. and Remote Sensing*, 2010, submitted. [Online]. Available: http://eches.perso.enseeiht.fr